



## RAPID COMMUNICATION

# Role of lncRNA *MALAT1* in UVA-induced corneal endothelial senescence



The corneal endothelial monolayer is responsible for maintaining corneal transparency through its barrier and pump functions. Endothelial cells do not proliferate *in vivo*, and aging-related reductions in cell density make the endothelium fragile.<sup>1</sup> However, the molecular mechanism associated with the aging corneal endothelium remains elusive. In this study, we used ultraviolet A (UVA)-light-induced senescence to mimic the degenerative endothelial changes during aging. *MALAT1*, the most abundant long non-coding RNA (lncRNA) gene in the cornea, was markedly down-regulated after UVA irradiation. The inhibition or activation of *Malat1* expression genetically led to the aggravation or remission of the cellular aging phenotype after UVA irradiation. Furthermore, an *in vitro* model established by the human corneal endothelial cell line (HCEC) recapitulated the morphological and molecular changes during aging, encouraging the investigation of the underlying mechanisms. We observed changes in the mitochondrial bioenergetic profiles of HCECs accompanied by extensive cell aging and reduced reproductive capacity after *MALAT1* was silenced by gene-targeting ASOs. Finally, *Malat1* knockout (KO) aggravated mouse corneal endothelial senescence and dysfunction, which reinforced our conclusions. Our findings indicate that *MALAT1* may contribute to the delay of aging processes involving endothelial cells and provide a new therapeutic target for treating aging-related corneal endothelium disorders.

To investigate the regulation of corneal endothelium aging, we generated a UVA-induced senescence mouse model using an established protocol.<sup>2</sup> The eyes of the mouse were irradiated with 500 J/cm<sup>2</sup> of UVA light and assessed one week later. No differences in the central corneal thickness and corneal clarity were detected (Fig. S2A, B). Furthermore, we performed senescence-associated  $\beta$ -galactosidase (SA- $\beta$ -gal) staining to identify the effects of UVA on the corneal endothelium. The UVA-

treated eyes showed more SA- $\beta$ -gal-positive cells than the controls, and the expression of the senescence markers *p16* and *p21* increased in the UVA-treated corneal endothelium (Fig. 1A, B; Fig. S1A). Immunohistochemical staining further validated the aging process of corneal endothelium after UVA irradiation (Fig. 1C, D). These results are consistent with the reports by previous studies that UVA light induces senescence in the corneal endothelium.

We next explored the relationship between lncRNAs and corneal endothelium aging. We analyzed the lncRNA profiles in our published single-cell RNA sequencing data of four human corneas derived from two normal individuals. Upon unsupervised clustering and t-distributed stochastic neighbor embedding (t-SNE), four primary cell types were annotated using classical specific markers (Fig. 1E; Fig. S3). *MALAT1* showed the highest expression across subtypes and was abundant in the top genes (Fig. 1F). Given the advancement of research on the function of lncRNAs in other cell types,<sup>3,4</sup> we determined the role of *Malat1* in regulating corneal-endothelium aging. The expression of *Malat1* was significantly down-regulated in the mouse corneal endothelium after UVA irradiation (Fig. 1G). Subsequently, RNA fluorescence *in situ* hybridization (FISH) showed that *Malat1* was expressed less in the UVA-treated corneal endothelium than in the controls (Fig. 1H). These observations indicated that *Malat1* may play a regulatory role in corneal endothelium senescence.

We proceeded to confirm the regulatory capacity of *Malat1* in corneal endothelial cells. Firstly, we knocked down *Malat1* in the mouse corneal endothelium by directly injecting *Malat1*-targeting short hairpin RNA (shRNA) (sh-*Malat1*) and negative control (sh-NC) into the anterior chambers (Fig. S4A). One week after irradiation, the knockdown of *Malat1* accelerated the aging process and cell loss in the corneal endothelium, as indicated by SA- $\beta$ -gal and junctional marker ZO-1 staining (Fig. 1I, J; Fig. S1B). Additionally, the sh-*Malat1* group showed higher *p16* and  $\gamma$ H2A.X expression than the controls (Fig. S5A).

Peer review under responsibility of Chongqing Medical University.

<https://doi.org/10.1016/j.gendis.2023.01.004>

2352-3042/© 2023 The Authors. Publishing services by Elsevier B.V. on behalf of KeAi Communications Co., Ltd. This is an open access article under the CC BY-NC-ND license (<http://creativecommons.org/licenses/by-nc-nd/4.0/>).

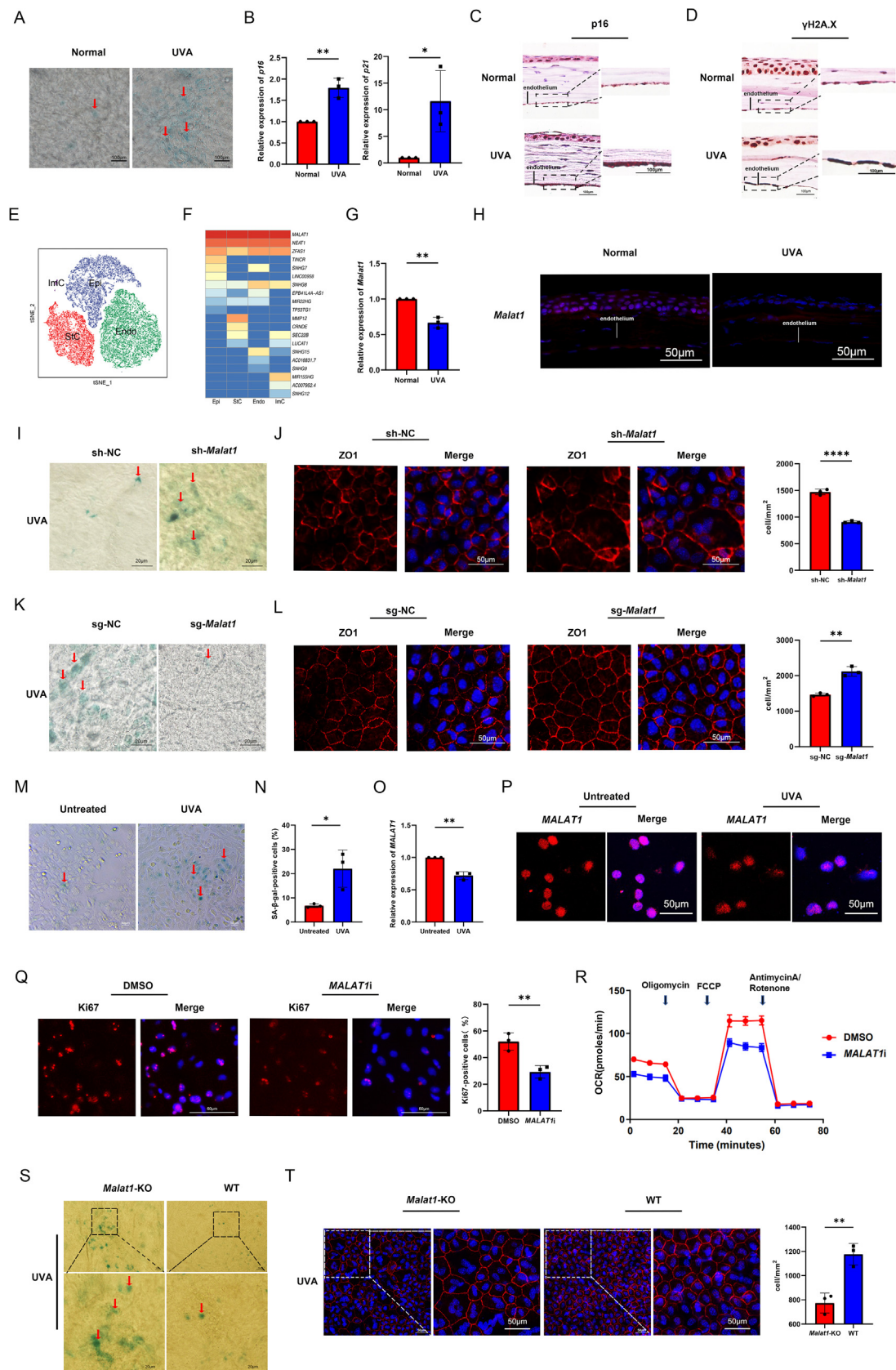


**Figure 1** MALAT1 was involved in UVA-induced corneal endothelial cell senescence. **(A)** Representative SA- $\beta$ -gal staining of the mouse corneal endothelium one week after UVA (the red arrows indicate senescent cells) ( $n = 3$ ) (scale bar = 100  $\mu$ m). **(B)** Relative mRNA levels of *p16* and *p21* upon UVA irradiation ( $n = 3$ ). **(C, D)** Representative immunohistochemical staining of *p16* and

These results indicated that *Malat1* deficiency made the corneal endothelium more susceptible to UVA irradiation. Next, we hypothesized that *Malat1* overexpression may protect the corneal endothelium from UVA damage. To test this, we used recombinant adeno-associated virus (rAAV) delivery of CRISPR activation to modulate the transcription of *Malat1* *in vivo*. *Malat1* was effectively up-regulated in the corneal endothelium of the *Malat1*-activated group (sg-*Malat1*) four weeks after the rAAV injection into the anterior chamber (Fig. S4B). We exposed the corneas of these mice to UVA irradiation and performed the same senescence detection used for sh-*Malat1*. An attenuated impairment was observed in the sg-*Malat1* group, implying greater functional preservation of the corneal endothelium than negative control (sg-NC) (Fig. 1K, L; Fig. S1C, 5B). Therefore, we speculated that *Malat1* played a critical role in protecting the mouse corneal endothelium from UVA-irradiation-related damage.

To identify the underlying process underlying *MALAT1*-regulation of cell function, we generated an *in vitro* senescence model.<sup>2</sup> HCECs were cultured to a confluent hexagonal monolayer before exposure to UVA light and recovery of 24 h in corneal endothelial cells media. The cells became senescent, which was indicated by marked SA- $\beta$ -gal staining and increased aging-related gene expression (Fig. 1M, N; Fig. S6A). Thereafter, quantitative real-time PCR (qRT-PCR) and FISH were carried out to quantify the transcription of *MALAT1*. As expected, UVA light compromised *MALAT1* expression (Fig. 1O, P; Fig. S6B). To elucidate the underlying molecular mechanism, we generated *MALAT1*-deficient (*MALAT1i*) HCECs using gene-targeting ASOs. Successful gene targeting was verified by qRT-PCR (Fig. S7A). *MALAT1* deficiency resulted in more SA- $\beta$ -gal-positive cells, which was consistent with the *in vivo* accelerated development of senescence phenotypes (Fig. S7B). Meanwhile, *MALAT1i* HCECs showed decreased proliferative activity through the nuclear expression of Ki67 24 h after UVA irradiation (Fig. 1Q), indicating that *MALAT1* is a geroprotective factor in HCECs. The endothelial cells were characterized by high bioenergetic needs as previously described,<sup>5</sup> and we determined whether *MALAT1*

accelerated corneal endothelium senescence via its effects on mitochondrial function. To this end, we assessed mitochondrial respiration through the measurement of the oxygen consumption rate (OCR) (Fig. 1R). Significant differences in mitochondrial basal respiration, ATP production, reserve capacity, maximal respiration, proton leak, and non-mitochondrial oxygen consumption were found between the control and *MALAT1i* HCECs (Fig. S8A–F). Collectively, the UVA-induced *MALAT1* down-regulation promoted senescence in HCECs, which may be regulated via mitochondrial function impairment.

Finally, we generated *Malat1* knockout mice to strengthen the relationship between *Malat1* reduction and corneal endothelium senescence. No obvious differences were observed in the general appearance and central corneal thickness of *Malat1* knockout and wild-type mice, except for a minimal loss in body weight (Fig. S9A–C). Subsequently, we subjected the controls and *Malat1* KO mice to UVA light and evaluated corneal endothelium changes using previously described senescence staining methods. As expected, *Malat1* gene deletion increased the percentage of SA- $\beta$ -gal-positive cells and expression of the senescence marker p16 and  $\gamma$ H2A.X after UVA irradiation (Fig. 1S; Fig. S1D, 9D). Additionally, greater variability in the cellular borders and a more significant reduction in cell density were observed in the *Malat1* KO mice (Fig. 1T). Taken together, these results confirm that *Malat1* deficiency aggravates UVA-induced senescence of the corneal endothelium.

A growing body of research has indicated that *MALAT1* is dysregulated and plays a significant role in the pathogenesis and development of various ocular diseases. We have demonstrated for the first time that the deficiency of *MALAT1* leads to severe corneal endothelium dysfunction during corneal endothelial aging through a pathologic process involving the mitochondrial signaling pathway. Functional gain via a CRISPR-activated adenoviral delivery system protects corneas from UVA-induced endothelial dysfunction. Thus, our findings identified *MALAT1* as a critical regulator of corneal endothelial aging, which improves our understanding of the complex biology of human corneal endothelial degeneration and the mechanism of action of lncRNA.

$\gamma$ H2A.X with or without UVA ( $n = 3$ ) (scale bar = 100  $\mu$ m). (E) t-SNE clustering of human corneal cells showing four distinct clusters differentiated by colors. (F) Heatmap of top lncRNAs for each subtype. (G) qRT-PCR analysis verified the expression of lncRNA *Malat1* in the mouse corneal endothelium treated with UVA ( $n = 3$ ). (H) FISH analysis of tissue sections stained for *Malat1* and counterstained with DAPI ( $n = 3$ ) (scale bar = 50  $\mu$ m). (I) Representative SA- $\beta$ -gal staining of the mouse corneal endothelium treated with control shRNA (sh-NC) and *Malat1* shRNA (sh-*Malat1*) upon UVA irradiation (the red arrows indicate senescent cells) ( $n = 3$ ) (scale bar = 20  $\mu$ m). (J) Representative confocal images of whole mounts of corneal endothelium showing ZO-1 staining and staining-based analysis for cell density ( $n = 3$ ) (scale bar = 50  $\mu$ m). (K) Comparison of SA- $\beta$ -gal staining images of UVA irradiated corneal endothelium treated with sg-NC, sg-*Malat1* (the red arrows indicate senescent cells) ( $n = 3$ ) (scale bar = 20  $\mu$ m). (L) ZO-1 staining showed corneal endothelium morphology after *Malat1* overexpression and staining-based analysis for cell density ( $n = 3$ ) (scale bar = 50  $\mu$ m). (M, N) SA- $\beta$ -gal staining with quantification of HCECs before and after UVA irradiation (the red arrows indicate senescent cells) ( $n = 3$ ) (scale bar = 50  $\mu$ m). (O) qRT-PCR analysis of *MALAT1* ( $n = 3$ ). (P) Stained for *MALAT1* transcripts and counterstained with DAPI in HCECs with UVA treatment ( $n = 3$ ) (scale bar = 50  $\mu$ m). (Q) Ki67 expression after the knockdown of *MALAT1* ( $n = 3$ ) (scale bar = 60  $\mu$ m). (R) The oxygen consumption rate curve for *MALAT1i* HCECs ( $n = 3$ ). (S) SA- $\beta$ -gal staining of the corneal endothelium of *Malat1* KO and wild-type mice (the red arrows indicate senescent cells) ( $n = 3$ ) (scale bar = 20  $\mu$ m). (T) Representative confocal images of the corneal endothelium showing ZO-1 staining and staining-based analysis for cell density ( $n = 3$ ) (scale bar = 50  $\mu$ m). The data are presented as mean  $\pm$  standard error; \* $P < 0.05$ , \*\* $P < 0.01$ , \*\*\*\* $P < 0.0001$  (two-tailed *t*-test).

## Author contributions

Q.W. and Q.Z. designed and supervised the study and acquired funding. Y.Q., Y.W., T.S., and C.D. carried out the experiments. S.D. and B.Z. analyzed the data. The manuscript was drafted by Y.Q. and Q.W., and reviewed and edited by Q.Z. All authors contributed to the article and approved the submitted version.

## Conflict of interests

All the authors declared no conflict of interests.

## Funding

This work was supported by the Taishan Scholar Program (No. tstp20221163), the Academic Promotion Program and Innovation Project of the Shandong First Medical University (China) (No. 2019RC008), the Natural Science Foundation of Shandong Province, China (No. ZR2019BH078), and the National Natural Science Foundation of China (No. 81800876, 82070927).

## Appendix A. Supplementary data

Supplementary data to this article can be found online at <https://doi.org/10.1016/j.gendis.2023.01.004>.

## References

- Joyce NC. Proliferative capacity of the corneal endothelium. *Prog Retin Eye Res.* 2003;22(3):359–389.
- Liu C, Miyajima T, Melangath G, et al. Ultraviolet A light induces DNA damage and estrogen-DNA adducts in Fuchs endothelial corneal dystrophy causing females to be more affected. *Proc Natl Acad Sci U S A.* 2020;117:573–583.
- Chen X, Hu J. Long noncoding RNA 3632454L22Rik contributes to corneal epithelial wound healing by sponging miR-181a-5p in diabetic mice. *Invest Ophthalmol Vis Sci.* 2021;62(14):16.
- Lu X, Ru Y, Chu C, et al. Lentivirus-mediated IL-10-expressing bone marrow mesenchymal stem cells promote corneal allograft survival via upregulating lncRNA 003946 in a rat model of corneal allograft rejection. *Theranostics.* 2020;10(18):8446–8467.
- Chen C, Zhang B, Xue J, et al. Pathogenic role of endoplasmic reticulum stress in diabetic corneal endothelial dysfunction. *Invest Ophthalmol Vis Sci.* 2022;63(3):4.

Yujie Qiao<sup>a</sup>, Bin Zhang<sup>a,b</sup>, Yani Wang<sup>a,b</sup>, Tian Sang<sup>a</sup>, Shengqian Dou<sup>a,b</sup>, Chunxiao Dong<sup>c,d</sup>, Qun Wang<sup>a,b,\*</sup>, Qingjun Zhou<sup>a,b,\*\*</sup>

<sup>a</sup> State Key Laboratory Cultivation Base, Shandong Provincial Key Laboratory of Ophthalmology, Shandong Eye Institute, Shandong First Medical University & Shandong Academy of Medical Sciences, Qingdao, Shandong 266071, China

<sup>b</sup> Qingdao Eye Hospital of Shandong First Medical University, Qingdao, Shandong 266071, China

<sup>c</sup> Qingdao University, Qingdao, Shandong 266071, China

<sup>d</sup> Eye Hospital of Shandong First Medical University (Shandong Eye Hospital), Jinan, Shandong 250021, China

\*Corresponding author. Shandong First Medical University, 5 Yan'erdao Road, Qingdao, Shandong 266071, China.

\*\*Corresponding author. Shandong First Medical University, 5 Yan'erdao Road, Qingdao, Shandong 266071, China. E-mail addresses: [wangqun8804@126.com](mailto:wangqun8804@126.com) (Q. Wang), [qjzhou2000@hotmail.com](mailto:qjzhou2000@hotmail.com) (Q. Zhou)

3 August 2022

Available online 21 April 2023